Nanoscale

Accepted Manuscript

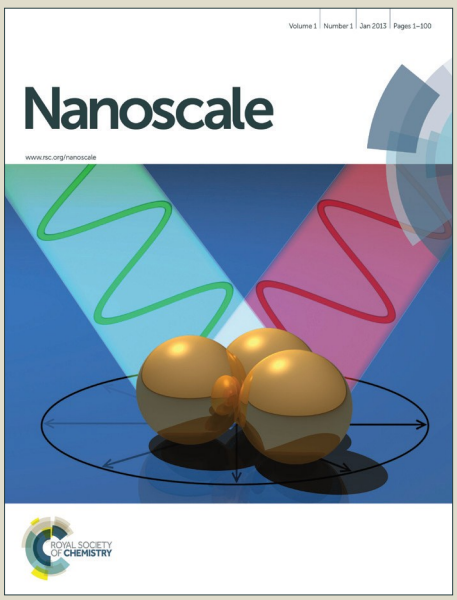

ROYAL SOCIETY OF CHEMISTRY

www.rsc.org/nanoscale

Nanoscale

ARTICLE

Novel Single Wall Carbon Nanotube (SWCNT) Functionalization Agent Facilitating *in vivo* Chemo/Thermo Combined Therapy

Received 00th January 2015,
Accepted 00th January 2015

DOI: 10.1039/x0xx00000x

www.rsc.org/

Liwen Zhang[a, †], Pengfei Rong[b, †], Minglong Chen[c], Shi Gao[c,*], Lei Zhu[a,*]

Carbon nanotubes (CNTs) have shown intriguing applications in biotechnological and biomedical fields due to their unique shape and properties. However, the fact that unmodified CNTs are prone to aggregation stunts CNTs applications in physiological conditions. In this research, we found as little as 1/5th the single wall carbon nanotube (SWCNT) weight of Evans Blue (EB) is capable of dispersing SWCNT as well as facilitating SWCNT functionalization. In the view of the binding between EB and albumin, the yielding product (SWCNT/EB) demonstrated extremely stability for weeks in physiologic conditions and can be endowed with a therapeutic ability by simply mixing SWCNT/EB with an albumin based drug. Specifically, the formed SWCNT/EB/albumin/PTX nanocomplex exhibits strong near-infrared (NIR) absorbance, and can be served as an agent for chemo/thermal therapeutic purpose. Our *in vivo* result reveals that SWCNT/EB/albumin/PTX after being administrated into the MDA-MB-435 tumor would effectively ablate tumor by chemo and photothermal therapy. Such combined treatment strategy provides remarkable therapeutic outcomes in restraining tumor growth compared to chemo or photothermal therapy alone. Overall, our strategy of dispersing SWCNTs by EB can be used as a platform for carrying other drugs or functional genes with the aid of albumin to treat diseases. The present study opens new opportunities in surface modification of SWCNT for future clinical disease treatment.

Introduction

Nanomaterials have attracted particular interest since their discovery [1-4]. Among them, carbon-based materials have shown great promise in diverse research fields. Specifically, single wall carbon nanotubes (SWCNTs), composed of a single graphene sheet that is rolled into a tubular structure, may have various advantages over other carbon nanomaterials. SWCNTs exhibit excellent physical and chemical properties such as strong optical absorbance [5, 6], extraordinary electrical/thermal conductivity [7] as well as a large surface area [8]. Due to the unique components and shape, SWCNTs hold many intriguing applications, especially in the biomedical field [9-13]. For example, SWCNTs are used in fluorescence [14], photoacoustic [5] and Raman imaging [15, 16] *in vitro* and *in vivo*. However, because they are easily driven by van der Waals forces and π-π interactions among themselves, unmodified SWCNTs are prone to aggregation[17, 18], which stunts their applications in physiological conditions like for molecular imaging or drug/gene/protein delivery.

With the help of surface engineering, it is now possible to minimize SWCNT aggregation by covalent or non-covalent modification based on a variety of biocompatible moieties. Non-covalent functionalization of SWCNTs imparts the nanotubes with adequate aqueous dispersibility, biocompatibility and improved targetability; but, as opposed to covalent modification, it also keeps the SWCNT structure intact. In the past decade, a number of strategies to effectively functionalize the large surface area (about 2600 m^2/g) of SWCNTs have been attempted [6, 19-22]. Specifically, surfactants, bearing a hydrophilic head and hydrophobic tail like nonionic Tween and ionic sodium dodecyl sulfate (SDS) [19, 23], are widely used for SWCNT dispersion [23]. Other SWCNT functionalization materials are amphiphilic molecules[24, 25], including phospholipid-poly(ethylene glycol) (PL-PEG) [2]. SWCNTs functionalized with amphiphilic molecules show excellent stability in the aqueous phase and can be easily modified for biomedical applications [11, 14, 26], such as tumor imaging, drug delivery, DNA/siRNA transfection and hyperthermia therapy. However, dispersion of SWCNTs by surfactants or amphiphilic molecules requires complex steps, making it difficult to endow biologically relevant functions onto SWCNTs. Another concern in current SWCNT dispersion methods is nonspecific absorption *in vivo*, where serum proteins can easily replace surfactants on SWCNTs and lead to poor biodistribution of SWCNTs. Recently, we reported the use of 5β-cholanic acid

[a] *State Key Laboratory of Molecular Vaccinology and Molecular Diagnostics & Center for Molecular Imaging and Translational Medicine, School of Public Health, Xiamen University, Xiamen 361005, China. E-mail: lei.zhu@xmu.edu.cn*
[b] *Department of Radiology, The Third Xiangya Hospital, Central South University, Changsha, Hunan 410013, China*
[c] *Department of Nuclear Medicine, China-Japan Union Hospital, Jilin University, Changchun, Jilin 130033, China. E-mail: gaoshi800830@163.com*
† These authors contributed equally.
* Corresponding authors.
Electronic Supplementary Information (ESI) available: Characterizations of EB dispersed SWCNT; Chemical structures of dyes applied for SWCNT dispersion; Spectrum of EB/Albumin; PTX loading efficiency onto albumin at different ratios. See DOI: 10.1039/x0xx00000x

modified hyaluronic acid nanoparticles (HANP) as an effective hydrophobic SWCNT carrier for PET/optical/PA imaging of SCC7 tumors *in vivo* [6]. The HANP/SWCNT complex demonstrated biocompatibility, cellular permeability and tumor targeting, but the stability of the complex *in vivo* needs to be further investigated.

In this work, we present a new SWCNT dispersion agent, Evans Blue (EB), an azo dye that has very high affinity to serum albumin. It is non-toxic[27, 28] and in most cases, EB is used to investigate the cardiac function after a myocardial infarction, cellular membrane permeability or vascular permeability in inflammatory diseases and cancer [29-33]. Herein, we found that as little as 1/5th the SWCNT weight of EB is capable of dispersing CNTs and can form a stable SWCNT/EB/albumin complex *in vitro* and *in vivo*. In the view of that the potential of albumin as a carrier [34, 35], we design to load an effective anti-cancer drug, paclitaxel (PTX), into albumin and then form a nanocomplex with the SWCNT/EB complex by simply mixing. We hypothesize that the SWCNT/EB/Albumin/PTX complex could provide combined chemo/thermal tumor therapy. The goal of the SWCNT/EB/Albumin/PTX nanocomplex is to a) stabilize SWCNT in aqueous solution; b) provide effective tumor-targeting by the Enhanced Permeability and Retention (EPR) effect; c) enable combined chemo/thermal therapy, while avoiding the potential drug-resistance of chemotherapy; and d) demonstrate an improved therapeutic effect over chemo or thermal monotherapy. Taking our *in vitro* and *in vivo* results together, we demonstrate that the SWCNT/EB/Albumin/PTX complex indeed effectively ablated tumors compared to either chemotherapy or photothermal therapy (PTT) alone. Moreover, our strategy of dispersing SWCNTs by EB can be used as a platform for carrying other drugs or DNA/siRNA with the aid of albumin to treat diseases. The present study opens new opportunities in surface modification of SWCNT for future clinical applications.

Experimental section

Reagents

NIR dye, Cy5.5-NHS, fetal bovine serum (FBS) and antibiotic were purchased from GE Healthcare (Pittsburgh, PA). Single wall carbon nanotube (SWCNT, Carbon>90%, >70% (carbon as SWNT), 0.7-1.3 nm diameter), was bought from Sigma Aldrich (St. Louis, MO). Dialysis bag and Dulbecco's Modified Eagle's Medium (DMEM) was obtained from Thermo Scientific (Waltham, MA). Hyaluronidase, MTT assay kit and 4,6-diamidino-2-phenylindole (DAPI) were purchased from Bioengineering Co., Ltd (Shanghai, China). Calcein-AM was obtained by Invitrogen (NY, USA). MDA-MB-435 (human breast cancer cell line) cells were obtained from ATCC (Manassas, VA). Glass bottom cell culture dishes were obtained from NEST Biotechnology Co. LTD (Nanjing, China). Eppendorf tubes (1.5 mL), 6-well chambers, 96-well flat-bottomed plates and cell culture dishes were purchased from JET BIOFIL (Guangzhou, China). All other chemicals were of analytical grade and used without further purification.

Preparation of dispersed single wall carbon nanotube

To coat SWCNTs by Evans Blue (EB), a 1:5 weight ratio of EB to SWCNT was used for dispersion in distilled water (DW). For example, 1 mg of short SWCNTs were dispersed in 0.2 mg of EB in 5 mL DW in a 15 mL Falcon tube. The solutions were then dispersed *via* probe-type sonication for 60 min at ~ 20 kHz with a 10 sec on / 1 sec off pulse sequence. To avoid over-heating, sonication was performed in an ice-water mixture bath. After sonication, the solution was subjected to centrifuge for 60 min (10, 000 rpm, 4ºC) to remove free CNT. The supernatant was added into ultrafiltration (cut off = 100 kDa) and centrifuged at 10000 rpm and 4 ºC for 10 min to free EB. The final product was concentrated and obtained.

Functionalization of SWCNT *via* EB coating

First, Albumin/PTX was prepared by High Pressure Homogenizer (PhD Technology International LLC, USA). Briefly, albumin (40 mg) and PTX (10 mg) were dissolved in ultrapure water (10 mL) and DMSO (1 mL), respectively. A mixture of albumin and PTX were homogenized for 15~20 min (20 000~25 000 psi) by High Pressure Homogenizer. The resulting solution was dialyzed against the excess amount of ultrapure water for 4 h. After being freeze-dried, albumin/PTX was obtained. Next, albumin/PTX was dissolved in a methanol/water solution (1/1, v/v) at concentrations of 1 mg/mL. The loading content and yield were confirmed by HPLC (C18, 5 µM, 250×4.6 mm) yielding 20% to 95% acetonitrile containing 0.1% TFA / ultrapure water containing 0.1% TFA over 40 min at a flow rate of 1 mL/min. Thirdly, a mixture of albumin/PTX (2 mL, 1 mg/mL) and SWCNT/EB (2 mL, 1 mg/mL) were stirred at room temperature for 30 min. After mixing, the products were purified by a disposal PD-10 column. Lastly, SWCNT/EB/albumin/PTX solution was incubated in a methanol/water solution (1/1, v/v) and centrifuged for 10 min (5000 rpm, 4 °C). The supernatant was collected and subjected to HPLC analysis. The loading efficiency of albumin/PTX onto SWCNT/EB was calculated according to a PTX standard curve.

Cell internalization

MDA-MB-435 cells at a density of 1×10^4 were seeded in a 6-well chamber at 37°C overnight. The next day, cells were washed with PBS and incubated with SWCNT/EB/albumin complex (100 µg/mL) at 37 °C and 5% CO_2 atmosphere for 3 h. In another group, SWCNT/EB/albumin was also added into MDA-MB-435 cells, but incubated at 4°C in order to verify albumin-mediated cell internalization. Free EB was used as control to further confirm SWCNT-mediated cell internalization. After incubation, cells were fixed in cold ethanol at -20 °C for 10 min. Lastly, cells were mounted with mounting medium containing DAPI for 10 min in the dark. Cell uptake of SWCNT/EB/albumin was observed by a confocal microscope (Leica, Germany) and the excitation and emission wavelengths were set at 580 nm and 700 nm for the EB/albumin formed complex[33].

***In vitro* drug release**

3 mL of SWCNT/EB/Albumin/PTX (1.65 mg of PTX) were dispersed in the dialysis bags (MWCO, 10 KDa). The dialysis bags were completely submerged in 15 mL of PBS (phosphate buffer solution, pH 7.4) containing 0.1% (v/v) Tween 80, which were respectively incubated at 37 °C and 50 °C under 100 rpm min-1. At determined time intervals, 150 μL PBS was collected and an equal volume of PBS was replaced in the tube. The collected solution was centrifuged at 10000 rpm for 10 min at 4 °C. Then, the supernatant was analyzed by HPLC (Thermo Fisher Scientific, Waltham, USA) using a reverse-phase C18 column (50×4.6 mm, 5 μm). The mobile phase was set a linear gradient of 20% to 90% acetonitrile/water (0.1% TFA) for 30 min at 1 mL min-1 flow rate and the detection wavelength was 254 nm. Sample solution was injected with a volume of 20 μL. The HPLC was calibrated with standard solutions of 62.5 to 1000 μg mL−1 of PTX dissolved in acetonitrile/water (50:50 v/v) (correlation coefficient of R2 = 0.9997). Release of PTX from SWCNT/EB/Albumin/PTX was calculated according to the standard curve as described in supplemental information.

***In vitro* photothermal ablation test**

To test the photothermal effect, SWCNT/EB and EB solutions in 1.5 mL Eppendorf tubes were each irradiated with a NIR laser (808 nm, Stone laser, Shenzhen) at a power density of 1 W/cm^2 for 250 sec. The laser spot was adjusted to cover the entire sample surface at an area of about 1 cm^2. Real-time thermal imaging was recorded using a FLIR Ax5 camera (FLIR Systems Inc., Wilsonville, USA) and quantified by BM_IR software.

Cytotoxicity test

The MDA-MB-435 cells were cultured in DMEM/high glucose medium supplemented with 10% FBS and 1% antibiotic solution at 37 °C and 5% CO_2. MDA-MB-435 cells at a density of 1×10^4 cells/well were seeded in a 96-well flat-bottomed plate and incubated overnight. After being washed with PBS, the cells were incubated with SWCNT/EB/albumin and SWCNT/EB/albumin/PTX solutions at different concentrations for 24 h at 37 °C with 5% CO_2. Experimental groups were rinsed again with PBS and replaced with fresh DMEM culture medium (100 μL). Experimental groups were irradiated with the 808 nm laser at a power density of 0, 0.25, 0.5 and 1 W/cm^2 for 15 min, respectively. The laser spot was adjusted to cover each well. After irradiation, cells were incubated in 37 °C with 5% CO_2 for another 24 h. Cell viability was evaluated by MTT assay.

Calcein AM/PI staining

MDA-MB-435 cells were seeded in a glass bottom cell culture dish with a density of 1 × 10^5 cells and grown to 80-90% confluency. After being washed with PBS, MDA-MB-435 cells were incubated with SWCNT/EB/albumin or SWCNT/EB/albumin/PTX for 24 h. Next, MDA-MB-435 cells were washed with PBS three times and 1 mL of fresh culture medium was replaced in the cells. Cells in control groups were cultured in fresh DMEM medium at 37 °C without 808 nm laser irradiation. Experimental groups were irradiated with 808 nm laser at powers of 0.25, 0.5 and 1 W/cm^2 for 15 min respectively, followed by incubation for 2 h under identical conditions as the control groups. After fresh DMEM medium was removed, MDA-MB-435 cells in each group were treated with Calcein AM (4 μmol/L) and PI solutions (4 μmol/L) in PBS and incubated at 37 °C with 5% CO_2 for 30 min. At last, cells were washed three times with PBS and fluorescence images of cells were acquired by confocal microscopy (Leica, Germany).

***In vivo* PTT**

Animal experiments were conducted under protocols approved by Animal Care and Use Committee (CCACUCC) of Xiamen University. MDA-MB-435 cells (4 × 10^6 cells in 50 μL of PBS) were injected in athymic nude mice (seven weeks old, 16-18 g). The tumor-bearing mice were randomly divided into six groups: (a) PBS without laser, (b) ABX, (c) SWCNT/EB without laser, (d) SWCNT/EB with laser, (e) SWCNT/EB/Albumin/PTX without laser and (f) SWCNT/EB/Albumin/PTX with laser. When the tumor volume reached an average size of 100 mm^3, 100 μL of PBS, ABX, SWCNT/EB, and SWCNT/EB/Albumin/PTX were intratumorally injected into the tumor-bearing mice. SWCNT/EB/albumin/PTX was evenly injected to 5 sites in tumor area. The injection dose was controlled at 3 mg/kg of PTX in SWCNT/EB/albumin/PTX complex or equal amount of SWCNT. After 1 hour, the tumor sites of (b) and (d) were irradiated with the NIR laser (808 nm) at a power density of 0.5 W/cm^2 for 3 min. Meanwhile, thermal images in tumors were recorded using a FLIR Ax5 camera and quantified by BM_IR software. The mouse body weight was recorded. Tumor growth (volume change) was monitored using the following equation: tumor volume =A×B^2/2, in which A is the largest diameter and B is the smallest diameter [36]. Compared with the original tumor volume, the relative tumor volumes of all groups were calculated at 14 days after treatment. Histological changes in tumor tissues were evaluated using hematoxylin and eosin (H&E) staining.

Computational modeling

3D structure of a SWCNT was generated using TubeGen 3.4 software (http://turin.nss.udel.edu/research/tubegenonline.html). Chirality parameters *m* and *n* were set as 14 and 0, which determined the diameter as 1.1 nm and length as 14 nm. C-C bond length was set as 1.4210 Å. The structure of EB was optimized and minimized by molecular mechanics. EB was docked onto the SWCNT structure using AutoDock Vina, as reported previously with slight modifications [37]. A cubic box was built with 126 × 126 × 126 points around the SWCNT. Docking simulations were carried out and the lowest binding mode was predicted and listed.

Statistical analysis

Results were presented as mean ± SD. Statistical analysis was performed using one-way ANOVA followed by Bonferroni multiple comparison test. *, $P < 0.05$ was considered statistically significant.

Results and discussion

Preparation and characterization of dispersed single wall carbon nanotubes (SWCNTs)

SWCNTs were functionalized by mixing with EB and sonicated for 1 hour. By π-π stacking between the SWCNT and EB, water-insoluble SWCNTs were coated by EB and demonstrated improved solubility in aqueous solution. As show in Fig. 1a, different ratios between EB and SWCNTs were used for dispersion to determine the minimum amount of EB needed to disperse SWCNTs with over 50% recovery. In this optimization step, we found that EB at 1/5th the amount of SWCNTs (w/w) was able to disperse SWCNTs with a recovery efficiency up to 55%. A decrease in the amount of EB, also caused a decrease in the recovery efficiency of SWCNTs. EB at 1/10th the SWCNT amount caused the recovery efficiency to decrease to 40%, and an even lower recovery at 20% was measured with a 1:20 EB:SWCNT ratio (Fig. S1a). Compared with other CNT dispersion agents, a low amount of EB is needed to effectively disperse SWCNTs at a low cost with simple steps[38]. The dyes containing stable double bonds, for example Cy5.5 and FPI-774, are not able to disperse SWCNTs, even though they each have effective water solubility themselves (Fig. S2). UV-vis-NIR spectra of EB, SWCNTs, and SWCNT/EB complex are shown in Fig. 1b, demonstrating the tight binding between SWCNTs and EB. Transmission electronic microscopy (TEM) and atomic force microscopy (AFM) of SWCNT/EB (Fig. 1b and Fig. S1b) shows that SWCNTs keep their original shape, despite the EB coating, with good dispersion. To determine the stability of SWCNT/EB complex, we added 1 mg/mL of SWCNT/EB into PBS, cell medium and serum and monitored stability *via* UV-vis-NIR spectroscopy for over 20 days. According to the spectra (Fig 1. c), the SWCNT/EB complex is stable for more than 21 days. In view of tight binding between EB and albumin, the SWCNT/EB complex will be more stable in the present of albumin, which will be highly beneficial for physiological applications. Raman signals were also measured after EB was coated onto the SWCNT surface. From Fig. 1d, SWCNT/EB demonstrated strong characteristic peaks at ~1580 cm^{-1} and 2500 cm^{-1} (G band and G' band), suggesting the coating did not affect SWCNT properties and can be used as a label during Raman imaging. Computer modelling was applied for simulation the binding modalities of EB and SWCNT. Energy between EB and SWCNT was calculated and listed as in Table S1. The binding mode with the lowest energy was chosen to represent SWCNT/EB in our study (Fig. 1d). All these data suggest effective functionalization of SWCNTs without affecting the SWCNT property.

Cell internalization of SWCNT/EB mediated by albumin

Many anti-tumor drugs have to be internalized into cells to work efficiently. For example, PTX plays an important role in the prevention of cancer cell proliferation. Once the drug is in the cells, PTX stabilizes the microtubule polymer to disrupt tubulin- microtubule function during cell division. However, the low solubility of PTX (< 0.4 μmol/L) in water and lack of targetability significantly limits its clinical applications. As a proof-of-concept, we used SWCNT/EB/albumin as a carrier to deliver PTX into cancer cells for therapeutic purposes. It is well documented that EB binds serum albumin. Moreover, albumin is taken up into cells *via* Gp60 protein activation. Firstly, we measured the fluorescent signal after EB binds with albumin *in vitro* [32, 33]. As shown in Fig. S3, strong fluorescent signals (ex/em: 580/700 nm) were detected after albumin was bound with SWCNT/EB, while no fluorescent signals were observed from EB without albumin. Next, we monitored the cell uptake of SWCNT/EB/albumin in cells by confocal microscopy. As shown in Fig. 2, a strong intracellular fluorescent signal was observed suggesting the presence of SWCNT/EB/albumin complexes in the cells. The cell uptake of SWCNT/EB/albumin complexes was effectively inhibited when cells were cultured at low temperature, during which cell activity is low. We also monitored that EB itself cannot be effectively taken up by cells. Although some reports show that SWCNTs can deliver drugs or DNA into cells, internalization of SWCNT/EB/albumin complexes into cells by the Gp60 pathway is more effective with less damage to the cells.

Loading and characterization of SWCNT/EB/albumin/PTX complexes

Chemotherapy induces apoptosis or dysfunction of tumor cells to treat cancer, but it may also cause severe side effects or induce drug resistance after long term treatment at high doses. Alternatively, nanomaterials with strong near-infrared light absorption are able to convert photon energy into thermal energy, which can destroy tumor cells when temperatures reach over 42 °C, so called photothermal therapy (PTT). To improve treatment efficiency and overcome the potential of chemotherapy-induced drug resistance, we designed a strategy combining PTT and chemotherapy. First of all, PTX was loaded into albumin by sonication. The characterization and loading efficiency of PTX to albumin was confirmed by HPLC as shown in Table S2. Next, Albumin/PTX complex was loaded onto SWCNT/EB by simply mixing the two compounds together. Successful loading was confirmed by UV-vis-NIR spectrum as shown in Fig. S4. A new peak from albumin was found at 280 nm, suggesting binding of albumin onto SWCNT/EB. The diameters of SWCNT/EB, SWCNT/EB/albumin and SWCNT/EB/albumin/PTX were also measured and compared. A 20 ± 2.3 nm diameter enlargement was found after Albumin/PTX was loaded onto SWCNT/EB compared to that of SWCNT/EB/albumin, suggesting that PTX loading affects the diameter of SWCNT/EB/albumin (Fig. S4b). The loading efficiency of Albumin/PTX onto SWCNT/EB was analysed and shown as in Table S3.

***In vitro* photothermal test**

The photothermal property of SWCNT/EB was firstly tested under the influence of a NIR laser probe at an 808 nm wavelength. SWCNT/EB (0.35 mg/mL) demonstrated a rapid increase in temperature from 30° C to 90 °C in about 3 min

(808 nm laser power, 1 W/cm^2), suggesting its potential in ablating cancer cells (Fig. 3a). The amount of EB on SWCNTs did not affect the temperature increase significantly; although when excess EB was coated onto the SWCNTs, a decrease to 82 ^{o}C was detected in the maximum temperature. The photothermal property was examined on a concentration gradient of SWCNT/EB as show in Fig. 3b. Compared with EB, SWCNT/EB demonstrated a quick temperature increase after laser irradiation. The more SWCNT/EB that was irradiated, the higher the temperature it reached (Fig. 3c and d). For example, 20 μg/mL of SWCNT/EB can reach a temperature of 90 ^{o}C in about 3 min (808 nm laser power, 1 W/cm^2), while a temperature of only 80 ^{o}C is reached when 2.5 μg/mL of SWCNT/EB is irradiated with the same laser as above. The *in vitro* photothermal property was tested and confirmed by repeating the experiments for 3 times. These *in vitro* data indicate that the SWCNT/EB complex is an effective agent for PTT.

***In vitro* release profile studies**

The PTX release profile was determined by dialysis method. As shown in Fig. 4, PTX released faster at 50 ^{o}C than it released at 37 ^{o}C, suggesting the higher temperature may be benefit for PTX release from SWCNT/EB/Albumin/PTX complex. The release profiles in the higher temperature (74.5%±0.73%) indicates a relative rapid PTX release in the initial 12 hours, while the release of PTX at 37 ^{o}C (67.5%±1.02%) is asymptotic release that is typical for PTX- encapsulated nanocomplex[39, 40].

Cytotoxicity

In view of the strong absorbance in the NIR region and high thermal capacity of SWCNTs, the photothermal property of SWCNT/EB/Albumin was investigated by irradiation with a NIR laser probe at an 808 nm wavelength. The viability of MDA-MB-435 cells under different treatments was evaluated (Fig. 5). In the SWCNT/EB/Albumin group treated group, all most all cells were alive while some cells dead when they were subjected to 808 nm laser irradiation, suggesting SWCNT/EB/albumin was not toxic without laser irradiation (Fig. 5a). On the contrary, the SWCNT/EB/Albumin/PTX complex caused more cells dead even without laser illumination, and significant suppression of MDA-MB-435 cell proliferation can be observed in a dose-dependent manner compared to those of SWCNT/EB/albumin under the same laser irradiation (Fig. 5a and b), indicating that SWCNT/EB/Albumin/PTX mediated chemo/thermal therapy is more effective in tumor cells ablation. To further identify cell viability, we co-stained the cells with Calcein AM and PI to distinguish live cells (green) and dead cells (red). In the control group (SWCNT/EB/Albumin/PTX without laser irradiation), most cells were live. This indicates that PTX alone is not sufficient to kill MDA-MB-435 cells without laser irradiation. When the laser power increases in the SWCNT/EB/Albumin/PTX group, more cells are killed, as observed by the red fluorescent signals. These results suggest that combined chemo/thermal therapy with SWCNT/EB/Albumin/PTX is localized and efficient.

***In vivo* photothermal ablation test**

Based on the *in vitro* combined chemo/thermal effects seen in the SWCNT/EB/Albumin/PTX group, we next tested the feasibility of applying SWCNT/EB/Albumin/PTX *in vivo* for PTT in MDA-MB-435 tumors. SWCNT/EB/Albumin/PTX was intratumorally injected when the tumor size reached about 100 mm^3. Thermal images were recorded with an IR thermal camera to monitor the temperature increase in the tumor area. As shown in Fig. 6, the tumor temperature increased from 27.06 ± 1.1 ^{o}C to 49.5 ± 1.5 ^{o}C in 3 min after irradiation by an 808 nm laser at a power density of 0.5 W/cm^2, which is sufficient for ablating cancer cell growth. When the laser power density was adjusted to 1 W/cm^2, the local temperature of the tumors reached 57.1 ± 2.5 ^{o}C from original mouse body temperature. No obvious temperature increase was found in other parts of the mouse. The 808 nm laser alone could not locally increase the tumor temperature without the presence of our nanocomplex.

Lastly, we studied the combined chemo/thermal therapy effect of SWCNT/EB/Albumin/PTX *in vivo*. Because clinical PTT is mostly based on an invasive strategy using a special optical fiber, we considered a local injection of SWCNT/EB/Albumin/PTX clinically relevant. Mice bearing MDA-MB-435 tumor cells were randomly divided into six groups (n = 5 for each group). In the treatment group, we intratumorally injected SWCNT/EB/Albumin/PTX and irradiated the tumor region with an 808 nm laser at a power density of 0.5 W/cm^2. The control groups included: PBS injection without laser irradiation, SWCNT/EB/Albumin/PTX without laser irradiation, SWCNT/EB/albumin with laser irradiation (808 nm, 0.5 W/cm^2) and SWCNT/EB/albumin without laser irradiation. As shown in Fig. 7, tumors in the SWCNT/EB/Albumin/PTX-administrated group with laser irradiation were significantly ablated. On the contrary, the tumors that received SWCNT/EB/Albumin/PTX and underwent no laser irradiation only demonstrated a growth rate compared to the PBS or SWCNT/EB/albumin treated groups without laser irradiation. ABX prevented tumor growth, but could not effectively ablate tumors as seen when the same amount of SWCNT/EB/Albumin/PTX was injected. This suggests that even when a lower dose of chemotherapy is administered to the tumor, a greater anti-cancer effect can be seen using our nanocomplex. Overall, we demonstrated the therapeutic advantage of our combined photothermal and chemo-drug strategy. To further investigate the SWCNT/EB/Albumin/PTX-mediated PTT/chemotherapy effect, we harvested tumor tissues treated with SWCNT/EB/Albumin/PTX and SWCNT/EB/albumin with and without NIR laser irradiation. PBS and ABX treated tumors were harvested as well. Hematoxylin and eosin (H&E) staining of these tumors were conducted. As shown in Fig. 7c, significantly damaged tumor tissues were observed in the SWCNT/EB/Albumin/PTX treated group after laser irradiation. Our results uncover that chemo/thermal combined therapy is able to offer an effective cancer treatment response in animal models at low laser power densities and drug doses.

Therefore, it can reduce side effects and act as an alternative choice for those tumors that are prone to drug resistance.

Conclusions

In summary, a novel SWCNT dispersion agent was introduced and applied to design a chemo/thermal combined therapy platform. As little as 1/5th the SWCNT weight of EB is able to disperse SWCNTs with more than 60% recovery efficiency. Based on the strong binding between EB and albumin, the final SWCNT/EB/albumin complex is stable and ready for further functionalization. In our study, the SWCNT complexes were loaded with PTX and demonstrated an improved therapeutic effect over chemotherapy or PTT alone. Because of the advantages of combined therapy, the EB-modified SWCNTs can serve as an alternative strategy and platform to treat tumors and can be easily loaded with other drugs or functional genes with high efficiency and effects.

Acknowledgements

This work was supported by National Science Foundation of China (NSFC) (81201129, 51373144, 81271606 and 30900359), National High Technology Research and Development Program of China (863 Program) (No. 2014AA020708), Fundamental Research Funds for the Central Universities (No. 20720150064), Science Foundation of Xiamen City (No.3502Z20140045) and Science Foundation of Fujian Province (No.2014Y2004).

Notes and references

1. R. H. Baughman, A. A. Zakhidov and W. A. de Heer, *Science*, 2002, **297**, 787-792.
2. Z. Liu, W. Cai, L. He, N. Nakayama, K. Chen, X. Sun, X. Chen and H. Dai, *Nature nanotechnology*, 2007, **2**, 47-52.
3. Y. Wang, Z. Li, J. Wang, J. Li and Y. Lin, *Trends in biotechnology*, 2011, **29**, 205-212.
4. M. S. Muthu, D. T. Leong, L. Mei and S. S. Feng, *Theranostics*, 2014, **4**, 660-677.
5. A. De la Zerda, C. Zavaleta, S. Keren, S. Vaithilingam, S. Bodapati, Z. Liu, J. Levi, B. R. Smith, T. J. Ma, O. Oralkan, Z. Cheng, X. Chen, H. Dai, B. T. Khuri-Yakub and S. S. Gambhir, *Nature nanotechnology*, 2008, **3**, 557-562.
6. M. Swierczewska, K. Y. Choi, E. L. Mertz, X. Huang, F. Zhang, L. Zhu, H. Y. Yoon, J. H. Park, A. Bhirde, S. Lee and X. Chen, *Nano letters*, 2012, **12**, 3613-3620.
7. K. Yang, S. Zhang, G. Zhang, X. Sun, S. T. Lee and Z. Liu, *Nano letters*, 2010, **10**, 3318-3323.
8. R. Q. Long and R. T. Yang, *Journal of the American Chemical Society*, 2001, **123**, 2058-2059.
9. B. S. Harrison and A. Atala, *Biomaterials*, 2007, **28**, 344-353.
10. R. Kumar, M. Dhanawat, S. Kumar, B. N. Singh, J. K. Pandit and V. R. Sinha, *Recent patents on drug delivery & formulation*, 2014, **8**, 12-26.
11. A. Bianco, K. Kostarelos and M. Prato, *Current opinion in chemical biology*, 2005, **9**, 674-679.
12. K. S. Siu, D. Chen, X. Zheng, X. Zhang, N. Johnston, Y. Liu, K. Yuan, J. Koropatnick, E. R. Gillies and W. P. Min, *Biomaterials*, 2014, **35**, 3435-3442.
13. W. Shao, A. Paul, B. Zhao, C. Lee, L. Rodes and S. Prakash, *Biomaterials*, 2013, **34**, 10109-10119.
14. H. Hong, T. Gao and W. Cai, *Nano today*, 2009, **4**, 252-261.
15. Z. Liu, X. Li, S. M. Tabakman, K. Jiang, S. Fan and H. Dai, *Journal of the American Chemical Society*, 2008, **130**, 13540-13541.
16. A. A. Bhirde, G. Liu, A. Jin, R. Iglesias-Bartolome, A. A. Sousa, R. D. Leapman, J. S. Gutkind, S. Lee and X. Chen, *Theranostics*, 2011, **1**, 310-321.
17. R. Shvartzman-Cohen, E. Nativ-Roth, E. Baskaran, Y. Levi-Kalisman, I. Szleifer and R. Yerushalmi-Rozen, *Journal of the American Chemical Society*, 2004, **126**, 14850-14857.
18. S. Rana and J. W. Cho, *Nanoscale*, 2010, **2**, 2550-2556.
19. L. Jiang, L. Gao and J. Sun, *Journal of colloid and interface science*, 2003, **260**, 89-94.
20. M. C. Hersam, *Nature nanotechnology*, 2008, **3**, 387-394.
21. R. M. Williams, S. Nayeem, B. D. Dolash and L. J. Sooter, *PloS one*, 2014, **9**, e94117.
22. H. Mao, N. Kawazoe and G. Chen, *Biomaterials*, 2013, **34**, 2472-2479.
23. L. Vaisman, H. D. Wagner and G. Marom, *Advances in colloid and interface science*, 2006, **128-130**, 37-46.
24. A. Nish, J. Y. Hwang, J. Doig and R. J. Nicholas, *Nature nanotechnology*, 2007, **2**, 640-646.
25. Z. Liu, S. M. Tabakman, Z. Chen and H. Dai, *Nature protocols*, 2009, **4**, 1372-1382.
26. X. Liu, H. Tao, K. Yang, S. Zhang, S. T. Lee and Z. Liu, *Biomaterials*, 2011, **32**, 144-151.
27. H. L. Wang and T. W. Lai, *Scientific reports*, 2014, **4**, 6588.
28. P. W. Hamer, J. M. McGeachie, M. J. Davies and M. D. Grounds, *Journal of anatomy*, 2002, **200**, 69-79.
29. J. Moitra, S. Sammani and J. G. Garcia, *Translational research : the journal of laboratory and clinical medicine*, 2007, **150**, 253-265.
30. H. el-Sayed, S. R. Goodall and R. Hainsworth, *Clinical and laboratory haematology*, 1995, **17**, 189-194.
31. A. Manaenko, H. Chen, J. Kammer, J. H. Zhang and J. Tang, *Journal of neuroscience methods*, 2011, **195**, 206-210.
32. J. Klohs, J. Steinbrink, R. Bourayou, S. Mueller, R. Cordell, K. Licha, M. Schirner, U. Dirnagl, U. Lindauer and A. Wunder, *Journal of neuroscience methods*, 2009, **180**, 126-132.
33. H. Jaffer, I. M. Adjei and V. Labhasetwar, *Scientific reports*, 2013, **3**, 3117.
34. F. Kratz, *Journal of controlled release : official journal of the Controlled Release Society*, 2008, **132**, 171-183.
35. A. Wunder, U. Muller-Ladner, E. H. Stelzer, J. Funk, E. Neumann, G. Stehle, T. Pap, H. Sinn, S. Gay and C. Fiehn, *Journal of immunology*, 2003, **170**, 4793-4801.
36. J. D. Hoeck, A. Jandke, S. M. Blake, E. Nye, B. Spencer-Dene, S. Brandner and A. Behrens, *Nature neuroscience*, 2010, **13**, 1365-1372.
37. V. E. Kagan, N. V. Konduru, W. Feng, B. L. Allen, J. Conroy, Y. Volkov, Vlasova, II, N. A. Belikova, N. Yanamala, A. Kapralov, Y. Y. Tyurina, J. Shi, E. R. Kisin, A. R. Murray, J. Franks, D. Stolz, P. Gou, J. Klein-Seetharaman, B. Fadeel, A. Star and A. A. Shvedova, *Nature nanotechnology*, 2010, **5**, 354-359.

38. M. Skowronek, Roterman, L. Konieczny, B. Stopa, J. Rybarska, B. Piekarska, A. Gorecki and M. Krol, *Computers & chemistry*, 2000, **24**, 429-450.
39. D. V. Peralta, Z. Heidari, S. Dash and M. A. Tarr, *ACS applied materials & interfaces*, 2015, **7**, 7101-7111.
40. T. Yang, M. K. Choi, F. D. Cui, J. S. Kim, S. J. Chung, C. K. Shim and D. D. Kim, *Journal of controlled release : official journal of the Controlled Release Society*, 2007, **120**, 169-177.